

Alma Mater Studiorum Università di Bologna
Archivio istituzionale della ricerca

Visible-Light Assisted Covalent Surface Functionalization of Reduced Graphene Oxide Nanosheets with Arylazo Sulfones

This is the final peer-reviewed author's accepted manuscript (postprint) of the following publication:

Published Version:

Lombardi L., Kovtun A., Mantovani S., Bertuzzi G., Favaretto L., Bettini C., et al. (2022). Visible-Light Assisted Covalent Surface Functionalization of Reduced Graphene Oxide Nanosheets with Arylazo Sulfones. CHEMISTRY-A EUROPEAN JOURNAL, 28(26), 1-6 [10.1002/chem.202200333].

Availability:

This version is available at: <https://hdl.handle.net/11585/891405> since: 2022-07-26

Published:

DOI: <http://doi.org/10.1002/chem.202200333>

Terms of use:

Some rights reserved. The terms and conditions for the reuse of this version of the manuscript are specified in the publishing policy. For all terms of use and more information see the publisher's website.

This item was downloaded from IRIS Università di Bologna (<https://cris.unibo.it/>).
When citing, please refer to the published version.

(Article begins on next page)

This is the final peer-reviewed accepted manuscript of:

Lombardi, L.; Kovtun, A.; Mantovani, S.; Bertuzzi, G.; Favaretto, L.; Bettini, C.; Palermo, V.; Melucci, M.; Bandini, M. Visible-Light Assisted Covalent Surface Functionalization of Reduced Graphene Oxide Nanosheets with Arylazo Sulfones. *Chemistry – A European Journal* **2022**, 28 (26), e202200333.

The final published version is available online at:
<https://doi.org/10.1002/chem.202200333>

Terms of use:

Some rights reserved. The terms and conditions for the reuse of this version of the manuscript are specified in the publishing policy. For all terms of use and more information see the publisher's website.

This item was downloaded from IRIS Università di Bologna (<https://cris.unibo.it/>)

When citing, please refer to the published version.

Visible-Light Assisted Covalent Surface Functionalization of *rGO* Nanosheets with Arylazo Sulfones

Lorenzo Lombardi,^{‡[a b]} Alessandro Kovtun,^{‡[c]} Sebastiano Mantovani,^[c] Giulio Bertuzzi,^[a b] Laura Favaretto,^[c] Cristian Bettini,^[b] Vincenzo Palermo,^[c] Manuela Melucci,^{*[c]} and Marco Bandini^{*[a b]}

[a] L. Lombardi, Dr. G. Bertuzzi, Prof. M. Bandini
Dipartimento di Chimica "Giacomo Ciamician"
Alma Mater Studiorum - Università di Bologna
Via Selmi 2, 40126 Bologna, Italy
E-mail: marco.bandini@unibo.it
Twitter: @M_BANDINI_GROUP

[b] L. Lombardi, G. Bertuzzi, M. Bandini
Center for Chemical Catalysis - C3-
Via Selmi 2, 40126 Bologna, Italy

[c] A. Kovtun, S. Mantovani, L. Favaretto, C. Bettini, Dr. V. Palermo, Dr. M. Melucci
Istituto per la Sintesi e la Fotoreattività (SOF) - CNR
Via Gobetti 101, 40129 Bologna, Italy
E-mail: manuela.melucci@isof.cnr.it
These authors contributed equally to the work

Supporting information for this article is given via a link at the end of the document

Abstract: We present an environmentally benign methodology for the covalent functionalization (arylation) of *rGO* nanosheets with arylazo sulfones. A variety of tagged aryl units were conveniently accommodated at the *rGO* surface via visible-light irradiation of suspensions of carbon nanostructured materials in aqueous media. Mild reaction conditions, absence of photosensitizers, functional group tolerance, and high atomic fractions (XPS analysis) represent some of the salient features characterizing the present methodology. Control experiments for the mechanistic elucidation (Raman analysis) and chemical nanomanipulation of the tagged *rGO* surfaces are also reported.

The advent of graphene in early 2000 has revolutionized the impact of carbon nanoforams on countless scientific disciplines such as organic electronics, printable circuits, corrosion control/prevention, drug delivery, water purification systems, nanofabrication and advanced composites.^[1] In this segment, graphene oxide (GO) derivatives are playing a major role due to their unique chemical, mechanical and physical properties in transistors, research topics.^[2] The growing popularity of graphene-based materials has soon brought to the demand of sustainable and reliable synthetic protocols for their chemical modification in order to access tunable functionalities.^[3]

The current trajectories for the chemical surface modification of GO derivatives can be categorized in two main areas, namely: *covalent and non covalent functionalization*, that differ for the nature of the chemical interactions between the exposed carbon-based layers and the derivatizing agent.^[4] Although complementary *pro* and *cons* can be found in both approaches, the covalent decorative tools are frequently preferred, delivering more robust and durable materials with highly predictable properties. In addition, the methodology adopted in covalent functionalizations can be dictated by the composition of the carbon surface; as a matter of fact, where oxidized functional groups (i.e. alcohols, epoxides, carbonyls/carboxylic acids)^[3-5] are targeted in GO manipulations, the argently present Csp^2 domains are preferably exploited in more

reduced graphene type materials. Concerning the latter approach, the employment of chemical entities responsible for the generation of highly reactive radical intermediates via thermal, photochemical or electrochemical means, is essential for the formation of new C-C or C-X bonds.^[4e,6] This aspect still represents a marked motivation towards the implementation of this strategy to larger scales, due to the intrinsic hazard of the required radical precursors (i.e. diazonium salts, peroxides).^[7]

In pursuit of tackling this still pendant shortcoming and based on our recent findings dealing with synthetic photochemical methodologies,^[8] we document here a new visible light assisted arylation of GO derivatives with arylazo sulfones (1). Arylazo sulfones, of general formula $ArN_2SO_2R(Ar')$, are a class of still underexplored bench stable compounds, capable of delivering aryl radical species upon visible light exposure.^[8d,9] Additionally, being generally deeply colored, the use of photosensitizers (PSs) is not required, with a consequent significant improvement of the operating conditions. The latter aspect should be carefully pondered since the structural affinity of common visible light PSs (π conjugate systems) and the π domains of the *rGO* planes could cause a detrimental aggregative interaction between the two species, precluding the desired energy transfers from the PS and the aryl radical precursors.^[10] As a consequence, the use of light for the covalent functionalization of graphene materials has been reported only sporadically, with a net predominance of energetic demand using UV based activation modes.^[11]

In the present study, *rGO* nanosheets were functionalized with differently substituted arenes under (photo)catalyst free conditions, via direct visible light irradiation and using arylazo sulfones as the source of radicals. Figure 1 summarizes the main features on the use of substrates 1.

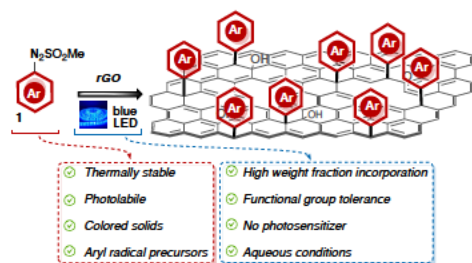


Figure 1. Schematic representation of the present visible-light assisted covalent arylation of *rGO* with arylazo sulfones 1

At the outset of our investigation, we focused our attention on reduced graphene oxide (*rGO*) due to the larger abundance of π domains present in the surface layers, with up to 75% of sp^2 hybridized C, as highlighted by the C 1s XPS signature analysis. Amongst the combination of high reproducibility and high atomic incorporation on the *rGO* surface, a survey of reaction conditions (stoichiometric ratio, light source/power, irradiation time and reaction media) was carried out in the conjugation of deep yellow (*p*-C₆H₄)N₂SO₂Me **1a** and *rGO*.^[12]

Conveniently, the incorporation of the *p*-chlorophenyl unit onto the *rGO* surface (O/C = 0.16 ± 0.01 , C (%) = 0.2 ± 0.01 , F (%) = , N (%) = , S (%) = , Figure 2 blue line) was quantitatively determined via XPS analysis (C 2p_{3/2} energy binding energy = 200.2 eV).^[13a]

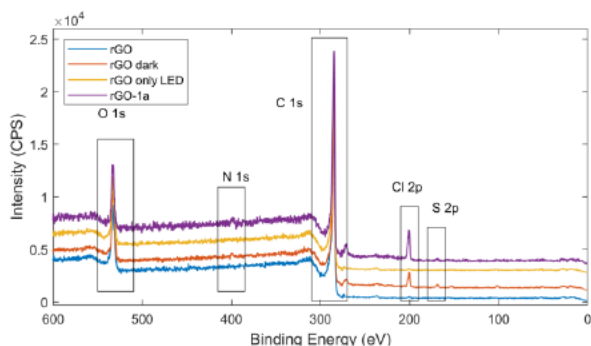


Figure 2. XPS survey spectra of reaction condition: pristine *rGO* (blue line) *rGO* (*rGO* dark (orange line) *rGO* with no reagent and only LED (*rGO* only LED (yellow line) *rGO*-1a (purple line) inset XPS Cl 2p signal. Constant was added to each spectrum for clarity

Acetonitrile was initially chosen as the reaction medium to guarantee a complete solubilization of **1a** with consequent maximization of the photoabsorption. A blue LED stripe, ("photochemical well" mode, 461 nm, 23 W, irradiation distance ≈ 10 cm, Figure 3b) was employed to exploit the absorption tail of **1a** in the visible light blue region (400–500 nm, $n\pi^*$).^[9a,14]

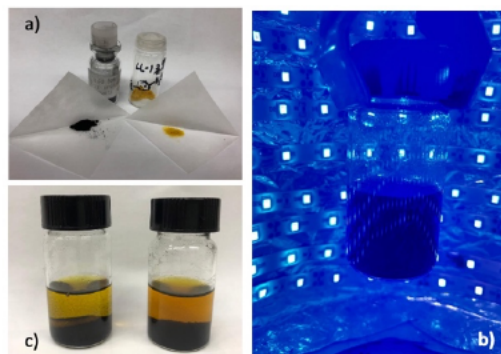


Figure 3. a) *rGO* (left) and arylazo sulfone **1a** (right) adopted as model substrates. b) The irradiation of the reaction mixture in the "photochemical-well" (blue-LED stripes 23 W). c) The reaction mixtures before (left) and after (right) irradiation

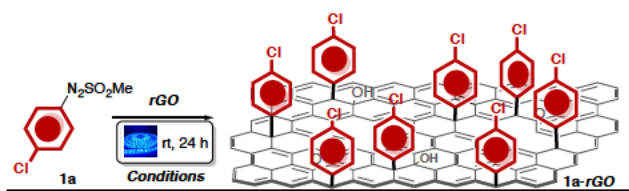
Under these conditions ([**1a**] = 0.05 M, **1a**: 0.1 mmol/6 mg *rGO*, rt, 24 h), **1a** *rGO* was recovered with a covalent incorporation of chlorine atoms with an atomic fraction = $2.8\% \pm 0.2$ (entry 2, Table 1) and without appreciable overall reduction of the carbon matrix (O/C = 0.14 ± 0.01) with respect to the pristine material (entries 1 and 6).^[15] Additionally, XPS analysis supports the presence of minor N and S contents, key deriving from photo-promoted decomposition of the arylazo sulfone (*vide infra* for mechanistic hypotheses).^[9d] In particular, while the S 2p_{3/2} signal found in the range of 168.1–168.8 eV, is in agreement with the SO₂ C group,^[16a] the N 1s signal at 399.4 eV is in perfect agreement with the C=N–N–C unit.^[16b]

Furthermore, exposure to a stronger irradiation source (40 W, 456 nm) did not provide any significant variation on the chemical outcome (entry 3), while the introduction of water in the reaction mixture (1:1 mixture with CH₃CN) was found to maximize reproducibility and probe incorporation ([C] = $4.8\% \pm 0.2$). This result can be rationalized by taking into account the capability of water to induce colloidal *rGO* suspensions.^[17] Based on this chlorine atomic fraction and since **1a** has 6 carbon atoms and 1 Cl atom (atomic fraction = 7), we could calculate the surface content of the *p*-C₆H₄ rings to be as high as $34\% \pm 3$ (see SI for further details).

The genuinely light-driven process was proved by running the reaction under the aforementioned conditions but in the dark (entry 5). Here, fixation of **1a** on the *rGO* surface probably via physisorption (*vide infra* for Raman analysis) worked in a significantly lower extent (2.4%).

In addition, the impact of the irradiation time on the *p*-C₆H₄ phenyl group incorporation was assessed by prolonging the reaction time up to 72 h (entries 7–9). However, the slight increase in % atomic fraction of chlorine atom detected ($5.0/5.1\% \pm 0.2$) testified that the covalent tagging occurred predominantly at the early stage irradiation time (entry 7).

Table 1. Optimization of the reaction conditions for the visible-light assisted covalent functionalization of *rGO* (for sake of clearness a single layer *rGO* was represented)



Run ^[a]	Conditions	O/C ^[b]	Atomic fraction [%] ^[b]	
			Cl	N/S
1	Pristine rGO	0.16	0.2 ± 0.1	-/-
2	23 W (461 nm) CH ₃ CN	0.14	2.8 ± 0.2	1.3/0.7
3	40 W (456 nm) CH ₃ CN	0.16	2.8 ± 0.2	0.9/0.6
4	23 W (461 nm) CH ₃ CN/H ₂ O	0.12	4.8 ± 0.2	0.8/0.4
5	dark CH ₃ CN/H ₂ O 24 h	0.18	2.4 ± 0.1	0.9/0.6
6	23 W (461 nm) CH ₃ CN/H ₂ O 24 h ^[c]	0.16	0.2 ± 0.1	-/-
7	23 W (461 nm) CH ₃ CN/H ₂ O 1 h	0.15	3.2 ± 0.2	0.8/0.7
8	23 W (461 nm) CH ₃ CN/H ₂ O 48 h	0.14	5.0 ± 0.2	0.9/0.5
9	23 W (461 nm) CH ₃ CN/H ₂ O 72 h	0.14	5.1 ± 0.2	1/0.5

[a] All the reactions were carried out in reagent grade solvents under air. **1a** = 0.1 mmol/6 mg of rGO. [**1a**] = 0.01 mM. When a solvent mixture was utilized a 1:1 mixture was employed. [b] O/C was determined via XPS from O 1s and C 1s signals. O/C ratios are expressed ± 0.01. Errors on N and S were ± 0.1. [c] in absence of **1a**.

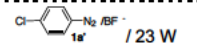
Once having established optimal conditions, the generality of the methodology was proved by subjecting a range of functionalized aryl azosulfones (**1b-q**) to blue LED irradiation in a suspension of rGO (H₂O:CH₃CN 1:1, Table 2). In particular, photoactive compounds featuring probe atoms for the XPS analysis such as halogens, nitrogen and sulfur, were selected in order to assess the covalent grafting at the surface, quantitatively.

The success of aryl functionalization on rGO surface was confirmed by XPS analyses, following the signature relative to the characteristic binding energy: C 2p, F 1s (Ar CF₃ at 687.8 eV and Ar F at 686.8 eV),^[13b] Br 3d_{5/2} (Ar Br at 70.1 eV,^[6d] N 1s (pyridine N at 398.8 eV) and I 3d_{5/2} (Ar I at 620.6 eV).^[13c] With concern to the S 2p_{3/2} signature, the thiophene-like C S C was identified from peak at 163.8 eV^[13d] well separated from the N SO₂ C residues (168 eV). A survey spectra are reported in the SI. Further confirmation of aryl functionalization can be found from the C 1s analysis, that evidenced peculiar chemical shifts of carbon atoms bonded to halogens (see SI).

From the data collected in Table 2 some conclusions can be drawn. The degree of oxidation on the rGOs confirmed not to be affected by the present photo-induced process, with a O/C ratio always ranking in the range of 0.13-0.19. The increase of oxygen atom content in entry 15 (O/C = 0.24) can be rationalized in terms of covalent grafting of the thiophene unit **1q** carrying the ester moiety. Analogously, the former rGO reduction recorded with compound **1q** (entry 16) is ascribable to the large number of carbon atoms present in the tagging triaryl unit.

Ar types of halogen atoms proved to be effectively tagged to the rGO surface via the aryl linkage. Additionally, the position of the halogen atom did not significantly affect the grafting, with the only exception of 2,4,6-Br₃(C₆H₂)N₂SO₂Me (**1l**, entry 11) and 2-I(C₆H₄)N₂SO₂Me (**1n**, entry 13).

Table 2. Generality of the protocol (for sake of clearness a single layer rGO was represented)

Run ^[a]	Ar (1)	O/C ^[b]	Atomic fraction % [X] ^[c]	Overall aryl [%] content ^[d]
1	3-Cl(C ₆ H ₄) (1b)	0.14	6.3 ± 0.4 [Cl]	38 ± 4
2	2-Cl(C ₆ H ₄) (1c)	0.14	6.2 ± 0.5 [Cl]	37 ± 5
3	3,5-Cl ₂ (C ₆ H ₃) (1d)	0.14	11.1 ± 0.8 [Cl]	33 ± 3
4	3-F(C ₆ H ₄) (1e)	0.16	4.4 ± 0.3 [F]	31 ± 3
5	4-F(C ₆ H ₄) (1f)	0.16	3.0 ± 0.3 [F]	21 ± 3
6	4-CF ₃ (C ₆ H ₄) (1g)	0.15	9.3 ± 0.5 [F]	31 ± 3
7	3,5-(CF ₃) ₂ (C ₆ H ₃) (1h)	0.16	11.0 ± 0.8 [F]	26 ± 3
8	4-Br(C ₆ H ₄) (1i)	0.15	5.8 ± 0.4 [Br]	40 ± 4
9	3-Br(C ₆ H ₄) (1j)	0.17	4.4 ± 0.3 [Br]	31 ± 3
10	2-Br(C ₆ H ₄) (1k)	0.13	5.3 ± 0.5 [Br]	37 ± 4
11	2,4,6-Br ₃ (C ₆ H ₂) (1l)	0.19	5.1 ± 0.4 [Br]	15 ± 2
12	4-I(C ₆ H ₄) (1m)	0.17	3.4 ± 0.3 [I]	24 ± 3
13	2-I(C ₆ H ₄) (1n)	0.17	1.5 ± 0.2 [I]	10 ± 2
14	3-pyridyl (1o)	0.15	3.9 ± 0.5 [N]	23 ± 3
15	1p	0.24	1.3 ± 0.2 [S]	13 ± 2
16	1q	0.07	6.9 ± 0.4 [S]	76 ± 4
17	 1a' / 23 W	0.16	1.0 ± 0.3 [Cl]	6 ± 1

[a] All the reactions were carried out in reagent-grade solvents under air. **1** = 0.01 mmol/6 mg of rGO. [**1**] = 0.01 mM. [b] Determined via XPS from O 1s and C 1s signal. O/C ratios are expressed ± 0.01. [c] Atomic abundance was obtained from Cl 2p, F 1s, Br 3d, N 1s and S 2p signals. [d] Overall aryl [%] content was calculated by multiplying the atomic abundance of X by the number of atoms composing the molecular probe attached to rGO and divided by the number of X atoms inside the correspondent molecule (see S).

In these cases, the corresponding **1l** rGO and **1n** rGO were so treated with slightly lower surface functionalizations (5.1% ± 0.5 of Br and 1.5% ± 0.2 of I, that correspond to 15% and 10% of overall aryl content, respectively). Additionally, not only monosubstituted but also disubstituted arenes (i.e. 3,5-C₂(C₆H₃))

1d and **3,5**-(CF₃)₂(C₆H₃) **1h**) were adequately accommodated onto the *r*GO surface with satisfying overall atomic fractions (11.1% of C and 11.0% of F, corresponding to 33% and 40% of overall content, respectively).

Worth mentioning, the 3-pyridyl ring was also effectively anchored to the *r*GO surface with a final 3.9% ± 0.5 N atom abundance (overall fraction = 23%) in the presence of 3-((methylsulfonyl)diazene)pyridine **1o** (entry 14). Finally, to further explore the possibility to conjugate the *r*GO matrix with functional heteroaryls, functionalization experiments were carried out in the presence of thienyl and benzimidazolones **1p** and **1q**. Satisfyingly, the incorporation of the thienyl scaffolds occurred in moderate to good extents (1.3–6.9%, entries 15 and 16).^[18]

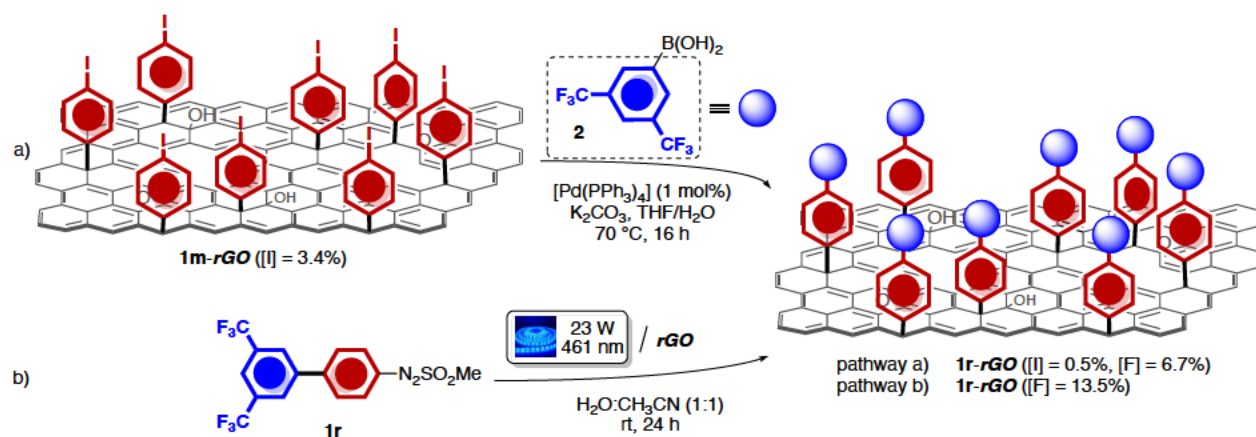
The complementarity of the presented methodology with the known diazonium salt based analogues^[6] was finally ascertained by treating a suspension of *r*GO with *p*-chlorophenyldiazonium salt **1a'** under conventional blue LEDs irradiation (entries 17). Interestingly, significant overtagging (1.0%) of the heterogeneous fragment was recorded proving the higher efficiency of our protocol.

Finally, the nanomanipulation of iodofunctionalized **1m** *r*GO was effectively proved by subjecting a **1m** *r*GO suspension

(THF/H₂O) to a palladium catalyzed Suzuki–Miyaura cross-coupling in the presence of commercial available boronic acid **2** (Scheme 1a).

XPS analysis of the recovered nanostructured material **1r** *r*GO (Figure 4) revealed an almost complete disappearance of the iodine signal (0.5 ± 0.1) in favor of the fluorine one (6.9%, F 1s at 688.3 eV), generated by the formation of the bis(trifluoromethyl)benzene group. The latter findings contribute to effect the methodology as a valuable converging synthetic tool for the preparation of tailored functional brushes on carbon based nanomaterials.

To further corroborate this chemical interpretation, we employed (CF₃)₂benzimidazolone **1r** in the photochemical derivatization of *r*GO (Scheme 1b). Gratifyingly, XPS analysis of recovered **1r** *r*GO showed a fluorine F 1s signal at 687.6 eV that is within the same range of the one recorded on **1r** *r*GO obtained via Suzuki coupling. Here, the higher atomic fraction of F = 13.5% vs 6.9% can be reasonably accounted by considering a partial degradation of **1r** *r*GO during the Pd-mediated nanomanipulation.



Scheme 1. a) Chemical elaboration of the tagged **1m-rGO** (Suzuki cross-coupling) b) Proving the consistency of the chemical elaboration of the covalently bound *p*-aryl units (Scheme 1a) via photo-irradiation of *r*GO with preformed compound **1r**

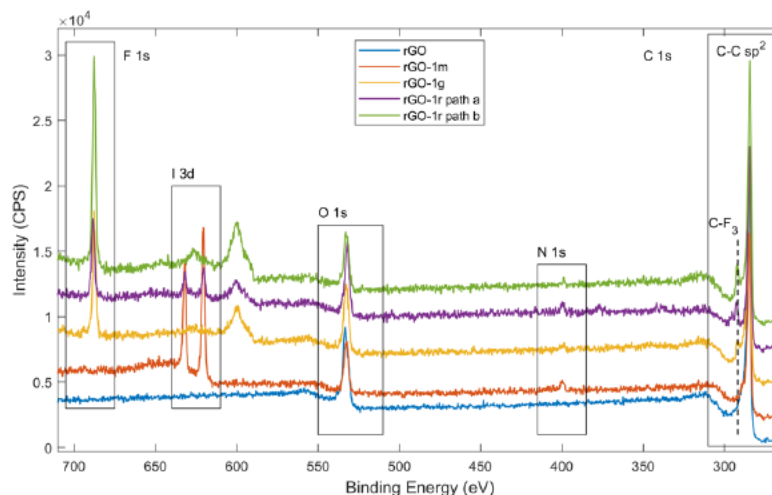
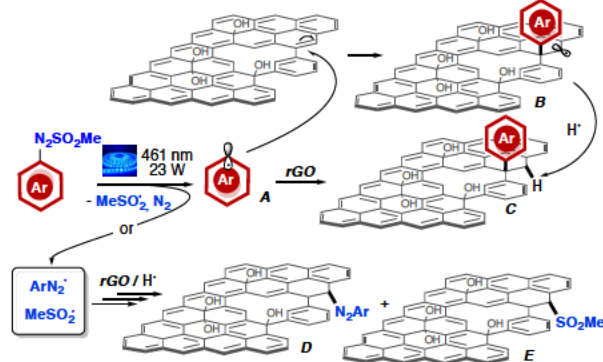


Figure 4. XPS survey spectra of reaction path proposed in Scheme 1. Pristine rGO (blue line), 1m-rGO (orange line), 1g-rGO (yellow line), 1r-rGO path a (purple line) and 1r-rGO path b (green line). F 1s, 3d, O 1s, N 1s and C 1s regions are highlighted by rectangles. C 1s region presents clear evidence of CF₃ carbon at 292 eV, which is chemically shifted from Csp² at 284.6 eV. Auger signal from F KLL is present in 650-600 eV region.

Mechanistically, the radical process depicted in Scheme 2 is proposed. In particular, the nitro radical of aryl azo sulfones with blue LEDs would lead to the corresponding aryl (A, Ar•) and methanesulfonyl radical via homolytic cleavage of the N-S bond and subsequent nitrogen extrusion from the firstly generated aryl diazenyl radical.^[9] Addition of the aryl radical A to the ππ unsaturation of the rGO surface would generate the covalent grafting of the aryl unit and consequent formation of a contiguous radical center B.^[19] Direct hydrogen abstraction from the medium would result in the tagged carbon species type C. Alternatively, trapping of either the methanesulfonyl radical or the electrocyclic aryl diazenyl radical before nitrogen loss by rGO can parallel the aryl at-on event, generating new heterofunctionalized "defects" on the nanostructure arylated lattice (see species D and E).

The afore-proposed hypothesis was partially verified by applying optimal conditions to the decoration of samples of GO with sulfone 1a (see SI for details). The amount of Csp² measured by XPS (C 1s signal) increases from 40% in GO to 75% in rGO. As expected, the manipulation of graphene oxide, that features a lower content of Csp² domains, led to a significant lower atomic fraction of C incorporation (1.4%) accompanied by a significant reduction of the carbonaceous material (see SI for details).^[15]



Scheme 2. Simplified mechanistic sketch

The afore-proposed hypothesis was verified both experimentally as well as spectroscopically. In particular, we applied the optimal conditions to the decoration of samples of GO with sulfone 1a (see SI for details). As expected, the manipulation of graphene oxide, that features a lower content of Csp² domains, led to a significant lower atomic fraction of C incorporation (1.4%) accompanied by a significant reduction of the carbonaceous material (see SI for details).^[15] In addition, the involvement of the Csp² domains in the present covalent grafting, was unambiguously proved by running a visible light treatment on HOPG (highly ordered pyrolytic graphite) with 1a. The spectra of 1a-HOPG samples obtained with and without light exposure were collected and reported in Figure 5. 1a-HOPG presents a clear D band at 1330 cm⁻¹ that demonstrates the formation of sp³ defects due to the covalent aryl at-on process on the Csp² composing the

surface of HOPG basal plane (change in hybridization from sp² to sp³). Conversely, no D peak was observed in absence of LED light on HOPG control sample (1a-HOPG dark), therefore, the light becomes a mediator than covalent grafting observed on 1a-HOPG sample in a light-driven process. G band (1582 cm⁻¹) and 2D band (2686 cm⁻¹) were also present (see SI). The ratio intensity of D and G band (I_D/I_G), was used as quantitative parameter of grafting efficiency, resulting 0.04 ± 0.01 for 1a-HOPG. The magnitude of I_D/I_G is compatible with a sub-monolayer coverage of diazenium moieties grafted on HOPG, as previously reported for electrochemical grafting^[6e] and chemistry activated grafting.^[20]

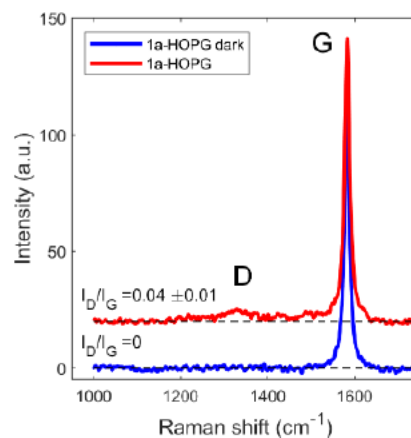


Figure 5. Raman spectrum of 1a-HOPG dark and 1a-HOPG. Linear background was subtracted and spectra were shifted for clarity.

In conclusion, we have documented a visible light-assisted covalent functionalization of rGO via an aryl at-on procedure. It is worth mentioning that: i) the absence of meta-based or organic PSs, ii) the very mild conditions employed (rt, aqueous media), iii) the wide functional group tolerance; iv) the dense surface decoration, and v) the quantitative analytical determination of the tagged aryl units via XPS, represent a unique combination of factors reflecting the present methodology as a viable synthetic alternative to the known protocols for the covalent modification of reduced graphene oxide surface. The late-stage functionalization of the modified rGO and a mechanistic proposal based on both experimental as well as spectroscopic (Raman) analyses completed the study. Efforts towards the implementation of the present protocol to the realization of different covalently conjugated nanostructured carbon materials are underway in our laboratories and will be presented in due course.

Acknowledgements

We are grateful to the University of Bologna for financial support and PRIN 2017 project 2017W8KNZW. The research leading to

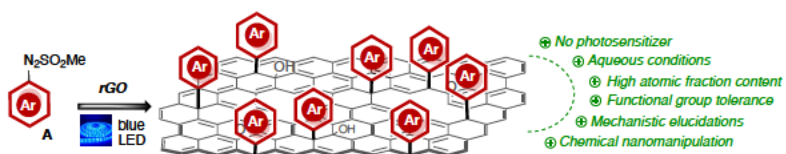
these results has received funding from the European Union's Horizon 2020 research and innovation programme under GrapheneCore3 881603 Graphene Flagship. Authors thank Prof. C. Zanard and "Centro Interdipartimentale Grand Strument" (C.I.G.S.) of Università di Modena and Reggio Emilia for the use of Raman equipment and to Dr. F. Bergamini for the precious technical assistance. A.K. thanks Dr. A. Candiani and Dr. D. Jones for the useful discussions. MB thanks Prof. Stefano Protti (UNIPV) for the stimulating discussions.

Keywords: rGO • surface modification • ary azasulfones • photochemistry • Suzuki cross coupling

- [1] a) A G Kelly T Hallam C Backes A Harvey A S Esmaily Godwin J Coelho V Nicolosi J Lauth A Kulkarni S Kinge L D A Siebbeles G S Duesberg J N Coleman *Science* **2017** 356 69-73 b) G Ersan O G Apul F Perreault T Karanfil *Water Res.* **2017** 126 385-398 c) F Perreault A F de Faria M Elimelech *Chem Soc Rev* **2015** 44 5861-5896 d) J Gao Y Feng L Jiang *Chem Soc Rev* **2017** 46 5400-5424 e) D S Chauhan M A Quraishi K R Ansari T A Saleh *Prog Org Coat* **2020** 147 105741 f) S Sattari M Adeli S Beyranvand M Nemati *Int J Nanomed* **2021** 16 5955-5980
- [2] a) D R Dreyer S Park C W Bielawski R S Ruoff *Chem Soc Rev* **2010** 39 228-240 b) D Chen H Feng J Li *Chem Rev* **2012** 112 6027-6053 c) R Hajian K Fung P P Chou S Wang S Balderston K Aran *Mat Matt* **2019** 14 37-44 d) S Obata K Saiki T Taniguchi T hara Y Kitamura Y Matsumoto *J Phys Soc Jpn* **2015** 84 121012 e) A Criado M Melchionna S Marchesan M Prato *Angew Chem Int Ed* **2015** 54 10734-10750 f) P Zheng N Wu *Chem Asian J* **2017** 12 2343-2353 g) Z Gu S Zhu L Yan F Zhao Y Zhao *Adv Mater* **2019** 31 1800662 h) G Reina J M González-Domínguez A Criado E Vázquez A Bianco M Prato *Chem Soc Rev* **2017** 46 4400-4416 i) A Vacchi C Menard-Moyon A Bianco *Phys Sci Rev* **2017** 20160103
- [3] For general review articles on the topic see a) J Liu J Tang J Gooding *J Mat Chem* **2013** 71 1201-1224 b) C Lai Y Sun H Yang X Zhang B Lin *Acta Chim Sinica* **2020** 78 877-887 c) S P Lonkar Y S Deshmukh A A Abdala *Nano Res* **2015** 8 1039-1074 d) D D Dreyer A D Todd C W Bielawski *Chem Soc Rev* **2014** 43 5288-5301 e) A Kasprzak A Zuchowska M Poplawska *Beil J Org Chem* **2018** 14 2018-2026 f) W Yu L Sisi Y Haiyan L Jie *RSC Adv* **2020** 10 15328-15345 g) M Minghao X Ming L Sijin *Acta Chim Sinica* **2020** 78 877-887 h) H Bingjie S Tao H Xiaoyu Y Mao Q Wenhao *Chin J Org Chem* **2020** 40 3279-3288 i) A Lopez J Liu *Adv Intell Syst* **2020** 2 2000123 j) A J Clancy H Au N Rubio G O Coulter M S P Shaffer *Dalton Trans* **2020** 49 10308-10318
- [4] a) J Liu J Tang J J Gooding *J Mat Chem* **2012** 22 12435-12452 b) S Eigler A Hirsh *Angew Chem Int Ed* **2014** 53 7720-7738 c) R Sekiya T Haino *Chem Asian J* **2020** 15 2316-2328 d) L Lombardi M Bandini *Angew Chem* **2020**, 132, 20951-20962 *Angew Chem Int Ed* **2020**, 59, 20767-20778 e) S Guo J Raya D Ji Y Nishina C Ménard-Moyon A Bianco *Nanoscale* **2020** 2 4085-4092 and references therein f) R Khan Y Nishina *Nanoscale* **2021** 13 36-50 g) Z A Jonoush M Farahani M Bohlouli Z Niknam A Golchin S Hatamie M Rezael-Tavirani M Omid H Zali *MiniRev Org Chem* **2021** 18 78-92 h) M Park N Kim J Lee M Gu B-S Kim *Mat Chem Front* **2021** 5 4424-4444
- [5] For representative examples of covalent conjugations of GO by exploiting oxidized functional groups see a) M Melucci E Treossi L Ortolani G Giambastiani V Morandi P Klar C Casirachi P Samor V Palermo *J Mat Chem* **2010**, 20 9052-9060 b) M Melucci M Durso M Zambianchi E Treossi Z-Y Xia Manet G Giambastiani L Ortolani V Morandi F De Angelis V Palermo *J Mat Chem* **2012** 22 18237-18243 c) M Durso A Borrachero-Conejo C Bettini E Treossi A Scidà E Saracino M Gazzano M Christian V Morandi G Tuci G Giambastiani L Ottaviano F Perozzi V Benfenati M Melucci V Palermo *J Mat Chem B* **2018**, 6 5335-5342 d) B Ranishenka E Ulashchik M Tatulchenkov O Sharko A Panarin N Dremova V Shmanai *FlatChem* **2021** 27 100235 e) S Mantovani S Khalifa L Favaretto C Bettini A Bianchi A Kovtun M Zambianchi M Gazzano B Casentini V Palermo M Melucci *Chem Commun* **2021** 57 3765-3768
- [6] For a collection of representative examples see a) C E Hamilton J R Lomeda Z Sun J M Tour A R Barron *Nano Lett* **2009** 9 3460-3462 b) A Sinitskii A Dimiev D A Corley A A Fursina D V Kosynkin J M Tour *ACS Nano* **2010** 4 1949-1954 c) J R Lomeda C D Doyle D V Kosynkin W-F Hwang J M Tour *J Am Chem Soc* **2008** 130 16201-16202 d) E Bekyarova M Etkis P Ramesh C Berger M Sprinkle W A de Heer R C Haddon *J Am Chem Soc* **2009** 131 1336-1337 e) J Greenwood T H Phan Y Fujita Z Li O Vasenko W Vanderlinden H Van Group W Frederickx G Lu K Tahara Y Tobe H Uji- S F L Mertens S De Feyter *ACS Nano* **2015** 9 5520-5535 f) Y Xia C Martin J Seibel S Eyley W Thielemans M van der Auweraer K S Mali S de Feyter *Nanoscale* **2020** 12 11916-11926 g) T Wei M Kohring M Chen S Yang H B Weber F Hauke A Hirsch *Angew Chem Int Ed* **2020** 59 5602-5606 h) Z Xia F Leonardi M Gobbi Y Liu V Bellani A Liscio A Kovtun R Li X Feng E Orgiu P Samor E Treossi V Palermo *ACS Nano* **2016** 16 7125-7134 i) D Hetemi V Noel J Pinson *Biosensors* **2020** 10, 4
- [7] D Bugaenko A A Volkov A V Karchava M A Yurovskaya *Russ Chem Rev* **2021** 90 116-170
- [8] a) E Marchi R Sinisi G Bergamini M Traghi M Monari M Bandini P Ceroni, *Chem Eur J* **2012** 18 8765-8773 b) E Marchi M Locritani M Baroncini G Bergamini R Sinisi M Monari C Botta W Mroz M Bandini P Ceroni V Balzani, *J Mat Chem C* **2014** 2 4461-4467 c) Q-Q Yang M Marchini W-J Xiao P Ceroni M Bandini, *Chem Eur J* **2015** 21 18052-18056 d) C Sauer Y Liu A De Nisi S Protti M Fagnogni M Bandini *ChemCatChem* **2017** 9 4456-4459 e) Y Liu A Parodi S Battaglioli M Monari S Protti M Bandini *Org Lett* **2019** 21 7782-7786 f) Y Liu S Battaglioli L Lombardi A Menichetti G Valenti M Montalti M Bandini *Org Lett* **2021** 23 4441-4446 g) S Battaglioli G Bertuzzi R Pedrazzani J Benetti G Valenti M Montalti M Monari M Bandini *Adv Synth Catal* **2022** 364 720-725
- [9] a) S Crespi S Protti M Fagnoni *J Org Chem* **2016** 81 9612-9619 b) P E da Silva Junior H M Amin A M Nauth F da Silva Emery S Protti T Opatz *ChemPhotoChem* **2018**, 2 878-883 c) J Liu M Tian Y Li X Shan A Li K Lum M Fagnoni S Protti X Zhao *Eur J Org Chem* **2020** 7358-7367 d) J Médard P Decorse C Mangeney J Pinson M Fagnoni S Protti *Langmuir* **2020** 36 2786-2793 e) A Li Y Li J Liu J Chen K Lu D Qiu M Fagnoni S Protti X Zhao *J Org Chem* **2021** 86 1292-1299
- [10] a) H-X Wang K-G Zhou Y-L Xie J Zeng N-N-Chai J Li H-L Zhang *Chem Commun* **2011** 47 5747-5749 b) A Wang W Yu Z Huang F Zhou J Song Y Song L Long M P Cifuentes M G Humphrey L Zhang J Shao C Zhang *Sci Rep* **2016** 6 23325
- [11] a) B Li L Zhou D Wu H Peng K Yan Y Zhou Z Liu *ACS Nano* **2011** 5 5957-5961 b) A Lundstedt R Papadakis H Li Y Han K Jorner J Bergman K Leifer H Grennberg H Ottosson *Small Meth* **2017** 1 1700214 c) R Papadakis H Li J Bergman A Lundstedt K Jorner R Ayub S Haldar B O Jahn A Denisova B Zietz R Lindh B Sanyal H Grennberg K Leifer H Ottosson *Nat Commun* **2016** 7 12962 d) A Piñeiro-García S M Vega-Díaz F Tristán D Meneses-Rodríguez G J Labrada-Delgado V Semetey *Ind Eng Chem Res* **2020** 59 13033-13041
- [12] Commercially available partially reduced rGO was directly employed in the surface modification reactions
- [13] a) D T Clark D Kilcast D B Adams W K R Musgrave *J Electron Spectrosc Relat Phenom* **1975** 6 117-134 b) F Le Floch M Matheron F Vinet *J Electroanal Chem* **2011** 660 127-132 c) M-C Bernard A Chausse E Cabet-Deliry M M Chehimi J Pinson F Podvorica C Vautrin-UI *Chem Mater* **2003** 15 3450-3462 d) J E Lyon A J Cascio M M Beerbom R Schlaf *Appl Phys Lett* **2006** 88 222109
- [14] S Protti D Ravelli M Fagnoni *Photochem Photobiol Sci* **2019** 18 2094-2101

-
- [15] Graphene oxide has been demonstrated to undergo visible-light photodisproportionative reduction via CO₂ releasing event see W-C Hou Chowdhury D G Goodwin Jr W M Henderson D H Fairbrother D Bouchard R G Zepp *Environ Sci Technol* **2015** 49 3435-3443
- [16] a) M Doring E Uhlig V Nefedov V Salyn *ZAAC* **1988** 563 105-115 b) T Yoshida S Sawada *Bull Chem Soc J* **1975** 48 345-346
- [17] a) D Konios M M Stylianakis E Stratakis E Kymakis *J Colloid Interface Sci* **2014** 430 108-112 b) S Park J An Jung R D Piner S J An X Li A Velamakanni R S Rouff *Nano Lett* **2009** 9 1593-1597
- [18] The high overall aryl content in **1q-rGO** can be explained by considering the length of the thiophene chain since the probe depth of XPS for carbon is about 6-7 nm and the **1q** covers most of *rGO* surface with 3 aromatic rings the XPS signal from the *rGO* in **1q-rGO** is more attenuated See a) L Pasquali F Terzi R Seeber S Nannarone D Datta C Dablemont H Hamoudi M Canepa V A Esaulov *Langmuir* **2011** 27 4713-4720 b) A L Bramblett M S Boeckl K D Hauch B D Ratner T Sasaki J W Rogers Jr *Surf Interface Anal* **2002** 33 506-515
- [19] Other possible quenching modalities of the radical intermediate **B** such as i) SET process with formation of a stabilized carbocation and subsequent restoring of the insaturation on the surface via deprotonation and ii) radical-radical coupling between **B** and a second Ar• species were not depicted in the Scheme 2 for clarity
- [20] M C Rodriguez González A Brown S Eyley W Thielemans K S Mali S De Feyter *Nanoscale* **2020** 12 18782-18789

Entry for the Table of Contents



Lightning @ surface. The visible light irradiation of unarmful and photoaberrant aryl azo sulfonates enabled the efficient covalent decoration (i.e. arylation) of rGO surfaces under mild, functional group tolerant and photosensitizer free conditions (see Scheme). Nanomanipulation of the tagged rGO surface via Pd catalyzed cross coupling was also documented.